MODELING OF INTERMITTENT CONVECTIVE DRYING OF WALNUTS IN SINGLE LAYER AND ITS INFLUENCE ON DEEP BED DRYING SIMULATION

by

Djordjije D. DODER* and Damir D. DJAKOVIĆ

Department of Energy and Process Engineering, Faculty of Technical Sciences,
University of Novi Sad, Novi Sad, Serbia

Original scientific paper
https://doi.org/10.2298/TSCI190120272D

This research concerns the convective intermittent drying of in-shell walnuts, as well as the comparison between intermittent and continuous regimes. The collected data from the continuous drying experiment served as the basis for the modeling of intermittent drying, where the kinetic semi-theoretical model was implemented. Mathematical model for the intermittent drying precedes the computer simulation and experimental procedure for a single layer. As the validity of the proposed model is confirmed, deep fixed bed drying simulation was included as well. Intermittent drying regimes with shorter tempering periods gave better results compared to the longer ones. Deep bed simulations showed that a fixed bed of walnuts should not be bigger than 15-20 cm.

Key words: *intermittent drying, walnuts, modeling, heat and mass transfer*

Introduction

Background

Walnut (*Juglans Regia L.*) is a very important foodstuff and its collection, drying, preservation and storage must be conducted with care. For many countries, such as the USA, China, Turkey, and Iran, walnut cultivation is a branch of agriculture with a very large production and export potential [1]. Walnut drying process in continuous regime has already been investigated in terms of thin-layer drying modeling for continuous regimes [2] and drying in deep bed [3]. At [4], heat capacity, thermal conductivity and thermal diffusivity of walnut kernels were investigated. Altuntas and Erkol [5] proposed the relations for estimating walnut physical characteristics, including density, bulk density and porosity. At [6] it is reported that initial moisture content of walnuts depends on variety, harvest time, and implementation of the ethephon chemical treatment.

Generally speaking, drying is a very energy-intensive process and big efforts to decrease energy consumption of such processes were made throughout the decades [7]. Convective drying principle (usually by using hot air as the drying agent) is one the most widely used even nowadays, when sophisticated and more efficient drying techniques are being implemented in large scale, such as microwave, infrared, vacuum and solar. Even so, convective drying is usually a desirable solution when the simplicity, feasibility and low investment costs rise as

* Corresponding author, e-mail: dj.doder@uns.ac.rs

the most influential factors when choosing an appropriate drier. However, convective driers usually work with lower energy efficiency in comparison to the others [8]. Energy consumption of walnut varieties could also be reduced by previous classification of walnuts with the similar size and moisture content, in order to avoid the unnecessary drying [9].

During the continuous convection drying, at some point concentration of moisture at the surface becomes too low, and the process efficiency decreases [10]. A process of dehydration where the tempering periods are inserted and the moisture content profile relaxation is allowed in those periods, is usually referred to as an *intermittent drying* process. It raises as one the most usable approaches when it comes to the energy saving issues or improving quality of dried materials [11]. Also, at [12] authors reported that intermittent oven drying of walnuts has more positive effects to product quality in comparison to direct oven drying and sun drying. Different approaches to mathematical modeling of intermittent drying can be found at [13], where authors claim that diffusion-based model gave the most accurate results. At [14], the intermittent drying in deep bed was modeled and the model involves the thin layer drying equation as the basis for the further calculation. Similar approach for deep bed simulation has been used for this research, where the model originally reported at [15] is adapted, then numerically interpreted and the obtained thin-layer drying equation is joined.

Investigation aims and drying regimes selection

The main aim was to propose an approach for modeling the process of intermittent walnuts drying, using the kinetic model, as well as to emphasize the energy saving possibilities. Later on, the justification of implementing an intermittent regime for deep bed drying was questioned.

Tempering period could last until the uniform moisture concentration profile is reached, but in practice, this period is typically much shorter. Relative humidity of drying air can also be periodically changed, but this approach is more energy intensive and is recommended only for the purposes of improving of a material quality [16]. Simultaneous lowering of both temperature and flow rate should result in the highest energy saving, but it might extend the total drying time significantly. Hence, this research is focused on the intermittent processes with periodical temperature lowering only, where the heater was turned off in certain periods (on/off regulation principle). The flow rate remained constant, as the fan was on all the time. Walnuts' drying is usually a long-lasting process, so every possibility for turning of the air heater could have significant results in terms of energy saving, if it does not affect the total drying time much. Product quality aspects are not under the scope of this research.

Walnuts should not be dried using temperatures higher than 43 °C, as the long-term exposure to higher temperatures could cause walnut oils to become rancid [5]. Thus, the highest drying temperature is limited to 40 °C. In continuous regime, walnuts were dried at 40 °C / 3 m/s, 30 °C / 3 m/s, 40 °C / 1 m/s, and 30 °C / 1 m/s, in order to derive a relation which is applicable for the wider range of temperatures and velocities. The case with temperature of 40 °C and air velocity of 3 m/s was taken as the reference for the later comparison with the intermittent regimes, because the highest drying intensity was expected for these parameters.

There are numerous ways to perform an intermittent drying. Based on the results from this research, the intermittency ratio of $t_{off}/(t_{on} + t_{off}) = 1/3$ was chosen, which means that the heater was turned on double the time it was turned off. As the 1/3 intermittency ratio was used, intermittent drying was carried out for two cases: *60 min on / 30 min off* and *30 min on / 15 min off*. In the end, the variable intermittency was investigated, in order to confirm the model validity for the wider range of intermittency ratios. During intermittent processes, temperature was periodically changed from 40 °C to 23 °C (the ambient air temperature).

Materials and methods

Walnut characteristics

The Fresh walnuts were collected in Vojvodina province, Serbia. Walnuts were carried in a mobile refrigerator, and stored in the laboratory refrigerator at the temperature of 9 °C, to prevent the occurrence of spontaneous drying caused by a high outdoor temperature. Before each experiment, walnuts were dehulled and cleaned manually. For this research, *Novosadski kasni* variety was used. All the samples had a similar size and the effective radius and initial moisture content was calculated as the average of 10 samples. For the purposes of calculation in this paper, the relations from [17] were used in order to relate the thermal and physical characteristics of *Novosadski kasni* walnut variety with its moisture content. Temperature dependences for these characteristics are neglected, because of the small temperature differences that appear in this type of process. Accordingly, the heat capacity, bulk density and thermal conductivity of a whole walnut were calculated as a function of moisture content only. Properties used for model calculation are presented in tab. 1 (during the calculation, all the mentioned properties of whole walnut vary, as the moisture content decrease):

Table 1. Properties used for model calculation [17]

Property	Components					
	Fat	Protein	Fiber	CH (other)	Ash	Water
ω [%]	64	14.83	4.98	14.04	1.93	variable
φ [%]	74.48	11.87	4.27	9.29	0.84	variable
C_p[kJkg^{-1}K^{-1}]	2.024	2.043	1.896	1.602	1.143	4.186
ρ [kgm^{-3}]	913.0	1314.3	1300.5	1589.7	2415.3	995.0
λ [Wm^{-1}K^{-1}]	0.1722	0.2122	0.2179	0.2391	0.3690	0.6150

Experimental set-up and procedure

Initial moisture content of walnuts was estimated by heating up walnut samples in the autoclave, at 130 °C, and holding it for at least 24 hours, according to [18], with the accompanying measuring of a sample mass. The results were confirmed by using the moisture analyzer *Precisa–XM60* (declared measurement readability 0.001-0.01%). The experimental facility set-up is placed at the Faculty of Technical Sciences, University of Novi Sad, Novi sad, Serbia. The installed electrical heater has the maximum power of 2000 W. Air is forced through the heater with a small fan, and then it enters the main axial fan *AB Electrolux Sweden – KS 5242/110* with installed power of 480 W. After that, hot air is pushed through the well-isolated main pipeline and flow equalizer, before it enters the layer of material which is subject to drying process. While the material is being dried, the balance *Mettler Toledo AG – PHS models – PH204S* (declared measurement readability 0.01%), registers the change in material mass and delivers the data to the computer unitwithin the predefined time intervals. For the temperature and air velocity measuring, the multifunctional anemometer device *Testo – 435* (declared measurement readability 0.01%), was used, while air relative humidity was measured by device with data logger *Testo – 177-H1*. The largest registered deviation during temperature measuring was ±0.7 °C, and during relative humidity measuring ±4%. Every single experiment was carried out with 50 similar samples in one layer, with the average mass of 12 g per sample. The collected data from the balance served as the starting point for the later analysis of drying process characteristics as the moisture removal rate is expressed through the change in product mass. Figure 1(a) shows the principal scheme of the facility in more detail, while fig. 1(b) shows the photography of the facility.

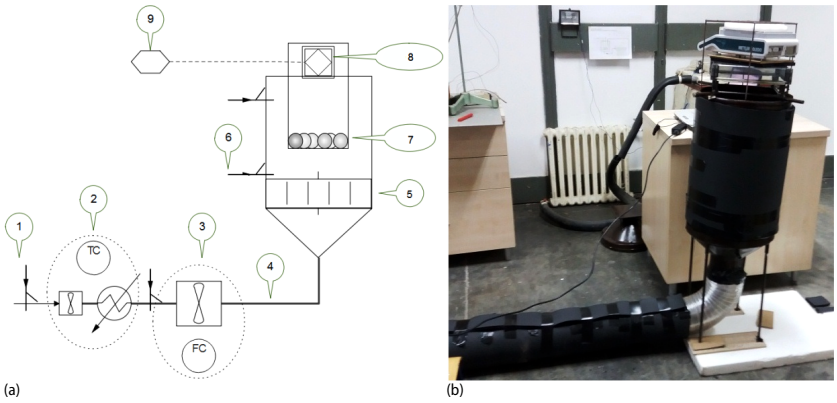

Figure 1. (a) Experimental facility; *1 – air inlet, 2 – temperature control unit (heater with small fan), 3 – flow control unit (main fan), 4 – pipeline, 5 – flow equalizer, 6 – temperature and air velocity measuring, 7 – material, 8 – balance, data logger, 9 – computer, data processing* **(b) facility photo**

Model description

Moisture removal kinetics for thin-layer

Moisture removal rate can be defined:

$$\frac{\mathrm{d}M}{\mathrm{d}t} = -k(M - M_\mathrm{e}) \tag{1}$$

Newton's TLD equation (or Lewis equation) represents the solution of differential eq. (1), and it is given in the non-dimensional form:

$$MR = \frac{M - M_\mathrm{e}}{M_i - M_\mathrm{e}} = \exp(-kt) \tag{2}$$

For the term k the next relation is set:

$$k = \frac{\pi^2 D_\mathrm{eff}}{r^2} \tag{3}$$

This way, the effective diffusivity term, D_eff, is introduced. If the effective radius, r, is known, eq. (3) is suitable for determining of D_eff, because term k can be easily calculated by using the linear regression procedure, similar as it is done at [19]. Arrhenius-type equation (for the calculation of effective diffusivity parameter) can be presented in its basic form [20]:

$$D_\mathrm{eff} = av^b \exp\left(-\frac{c}{T}\right) \tag{4}$$

Temperature term in this equation represents the internal temperature of walnut center.

Temperature distribution

Dimensionless numbers Biot number, α, Nusselt number, and Fourier number were calculated for the whole range of moisture content values. The Nu for spherical bodies can be calculated [21]:

$$\mathrm{Nu} = 2 + (0.43\,\mathrm{Re}^{1/2} + 0.06\,\mathrm{Re}^{2/3})\,\mathrm{Pr}_a^{0.4}\left(\frac{\mu_\mathrm{a}}{\mu_s}\right)^{1/4} \tag{5}$$

and the Prandtl number and μ are known at the air temperature.

According to the calculated values of Biot number, a walnut has to be analyzed as a body with non-homogenous temperature field. Hence, to simulate the temperature variations inside the walnuts, the approximate solution of heat equation for the non-stationary processes was used. The temperature of walnut center can be expressed in a non-dimensional form:

$$\theta_0^* = C_1 \exp(-\zeta_1^2\,\mathrm{Fo}) \tag{6}$$

Coefficients C_1 and ζ were taken from [21]. Also, it can be expressed as the temperature ratio:

$$\theta_0^* = \frac{T_\mathrm{a} - T_\mathrm{i}}{T_\mathrm{a} - T} \tag{7}$$

Deep bed equations

Modeling of deep bed drying was done in order to run the process simulation. Besides the eq. (2), which describes the drying kinetics, *i. e.* the moisture removal rate for every single space step of the bed, the equations for moisture balance, moist air energy balance and moist material energy balance were used, respectively [15]:

$$\left(\frac{\partial X}{\partial z}\right) = -\left(\frac{\rho_d}{G_\mathrm{a}}\right)\left(\frac{\partial M}{\partial t}\right) \tag{8}$$

$$\frac{\partial T_\mathrm{a}}{\partial z} = \frac{\left(-h_{cv} + C_{p,\mathrm{w}}\rho_d \dfrac{\partial M}{\partial t}\right)\left(T_\mathrm{a} - T_\mathrm{g}\right)}{Ga(C_{p,\mathrm{a}} + C_{p,\mathrm{w}}X)} \tag{9}$$

$$\frac{\partial T_\mathrm{g}}{\partial t} = \frac{h_{cv}(T_\mathrm{a} - T_\mathrm{g})}{\rho_d(C_{p,\mathrm{g}} + C_{p,1}M)} + \frac{\rho_d\left[L_\mathrm{g} + (C_{p,\mathrm{w}} - C_{p,1})T_\mathrm{g}\right]\left(\dfrac{\partial M}{\partial t}\right)}{\rho_d(C_{p,\mathrm{g}} + C_{p,1}M)} \tag{10}$$

The volumetric heat transfer relation was taken from [22], and when it is adjusted to SI metric system it can be calculated:

$$h_{cv} = \frac{12vT^{0.3}}{d^{1.35}}0.07 \tag{11}$$

Solution procedure

All the numerical calculations were done using MATLAB® programming language.

If logarithmic non-dimensional moisture content ln(MR) is set up versus drying time, the slope of the line will be equal to k, after which the D_eff is determined. After D_eff was determined for the every mentioned case, in order to develop the model in the form of the Arrhenius-type equation, the non-linear regression technique was used.

With Fourier number included, an iterative calculation can be applied for solving the eq. (6), for every time step. For the numerical interpretation, eq. (6) can be transformed to the following form:

$$T_{i+1} = T_{\mathrm{a},i+1} - (T_{\mathrm{a},i+1} - T_i)C_{1i} \exp\left(\frac{-\zeta_i^2 \lambda_i t}{\rho_i C_{p,i} r_i^2}\right) \tag{12}$$

Here, the values with i subscript represent the values for the current time step, and those with $i+1$ for the next time step. At first place, the matrix of MR values is set, where time steps are presented by the column index increment. In other words, one row is the array of the solutions of MR for every time step during the process, but for only one effective diffusivity value. Every row is then calculated for the different value of effective diffusivity. The matrix dimensions are 79×79, which, for the time step of 10 minute, represents the total drying time of 800 minute (initial time of 0 minute is also included). The calculation is repeated for 79 different diffusivities, which in essence are the results of 79 different temperatures, calculated for the same time steps. Figure 2(a) illustrates the initial matrix for the calculation and fig. 2(b) the resulting matrix with the first two relevant columns separated with the dashed line.

$$\begin{bmatrix} MR^0_{t=t(0)} = f(D_{eff\,0}) & MR^0_{t=t(1)} = f(D_{eff\,0}) & \cdots & MR^0_{t=t(n)} = f(D_{eff\,0}) \\ MR^1_{t=t(0)} = f(D_{eff\,1}) & MR^1_{t=t(1)} = f(D_{eff\,1}) & & \\ \vdots & & \ddots & \\ MR^{n-1}_{t=t(0)} = f(D_{eff\,n-1}) & & & MR^{n-1}_{t=t(n)} = f(D_{eff\,n-1}) \\ MR^n_{t=t(0)} = f(D_{eff\,n}) & & & MR^n_{t=t(n)} = f(D_{eff\,n}) \end{bmatrix}$$

(a)

$$\begin{bmatrix} MR^0_{t=t(0)} = f(D_{eff\,0}) = 1 & MR^0_{t=t(1)} = f(D_{eff\,0}) & \cdots & MR^0_{t=t(n)} = f(D_{eff\,0}) \\ MR^1_{t=t(0)} = f(D_{eff\,1}) \cdot MR^0_{t=t(1)} & MR^1_{t=t(1)} = f(MR^1_{t=t(0)}) & & MR^1_{t=t(n)} = f(MR^1_{t=t(n-1)}) \\ \vdots & & \ddots & \\ MR^{n-1}_{t=t(0)} = f(D_{eff\,n-1}) \cdot MR^{n-2}_{t=t(1)} & MR^{n-1}_{t=t(1)} = f(MR^{n-1}_{t=t(0)}) & & MR^{n-1}_{t=t(n)} = f(MR^{n-1}_{t=t(n-1)}) \\ MR^n_{t=t(0)} = f(D_{eff\,n}) \cdot MR^{n-1}_{t=t(1)} & MR^n_{t=t(1)} = f(MR^n_{t=t(0)}) & & MR^{n-1}_{t=t(n-1)} = f(MR^n_{t=t(n-1)}) \end{bmatrix}$$

(b)

Figure 2. (a) The initial matrix, (b) The resulting matrix

Further on, the initial MR is equal to 1. After all values in the initial matrix are calculated, the re-calculation procedure must take place. As one effective diffusivity value is relevant for one time step, the re-calculation is done as the first element of the second row is multiplied by the second element of the first row (which represent the MR value after 10 minute *i. e.* one time step). This way, the initial condition for the next row is changed, thus all the other values in the row will be changed accordingly. The procedure is then repeated for every row. Ultimately, the first and second element of every row in descending order, form the array of MR values for a particular process.

After the mentioned procedure is done, the resulting MR array is implemented into the deep bed model, which is solved using the numerical method of finite differences. Namely, for the maximum bed height of 60 cm, 1-D air-flow and 1800 minute of simulated drying time, the same time step Δt of 10 minute as for the thin-layer was taken, and the space step Δz was set to 1 cm. The simulation took around 20 hours to finish, using hardware Intel® i3-4130® 3.40 GHz with 4 GB of RAM. Figure 3 shows the procedure of calculation and the principal programming algorithm.

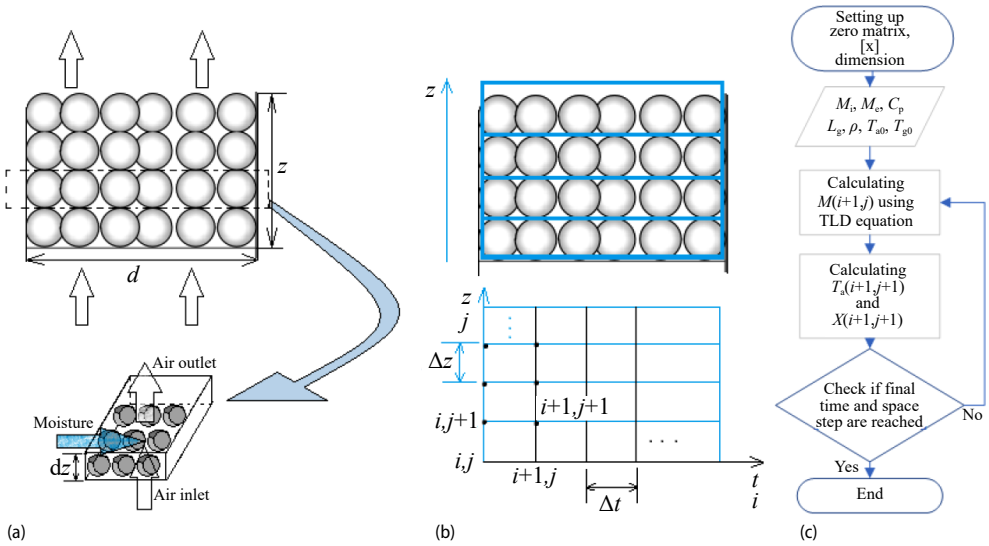

Figure 3. (a) Illustration of one layer of deep bed, (b) numerical grid, and (c) solution algorithm for deep bed

Equation (2) is numerically interpreted:

$$M_{(i+1)} = M_{(i)} \exp[-k_{(i)}(\Delta t)] + M_{e(i)}\{1 - \exp[k_{(i)}(\Delta t)]\} \tag{11}$$

where k for every time step is calculated using the obtained D_{eff} value for the relevant time step (the equation for calculating of D_{eff} is presented in the next chapter, as it is a part of the most important contributes achieved through this research). In similar fashion, eqs. (8)-(10) were interpreted:

$$X_{(i+1,j+1)} = X_{(i+1,j)} - \frac{\rho}{G_{\text{a}}}\left(\frac{M_{(i+1,j)} - M_{(i,j)}}{\Delta t}\right)\Delta z \tag{12}$$

$$T_{\text{a}(i+1,j+1)} = T_{\text{a}(i+1,j)} \exp\left[-\frac{\left(-h_{cv} - \rho C_{p\text{w}}\dfrac{\partial M}{\partial t}\right)}{G_{\text{e}}(C_{p,\text{a}} + C_{p,\text{w}}X)}\Delta z\right] + T_{\text{g}(i+1,j)}\left\{1 - \exp\left[-\frac{\left(-h_{cv} - \rho C_{p,\text{w}}\dfrac{\partial M}{\partial t}\right)}{G_{\text{a}}(C_{p,\text{a}} + C_{p,\text{w}}X)}\Delta z\right]\right\} \tag{13}$$

$$T_{\text{g}(i+1,j)} = T_{\text{g}(i,j)} \exp\left[-\frac{h_{cv}}{\rho(C_{p,\text{g}} + C_{p,1}M)}\Delta t\right] + \left(-\frac{h_{cv}}{\rho(C_{p,\text{g}} + C_{p1}M)}T_{\text{a}(i,j)} - \left\{\frac{\rho_d\left[L_{\text{g}} + (C_{p,\text{w}} - C_{p,1})T_g\right]\left(\dfrac{\partial M}{\partial t}\right)}{\rho_d(C_{p,\text{g}} + C_{p,1}M)}\right\}\right)\left\{1 - \exp\left[-\frac{h_{cv}}{\rho(C_{p,\text{g}} + C_{p,1}M)}\Delta t\right]\right\} + \frac{}{-\dfrac{h_{cv}}{\rho(C_{p,\text{g}} + C_{p,1}M)}} \tag{14}$$

Results and discussion

Thin-layer results

According to the measurements, M_i used for the calculation was 34%$_{d.b.}$. The M_e was taken to be 8%$_{d.b.}$ according to [5]. Every different drying temperature and air velocity took different time to achieve the M_e, but in order to get the convenient results for the further analysis, the calculation of effective diffusivity was done on the same time basis of 1000 minute. The statistical data was done for the analysis of fitting model compatibility with the curves. The chosen statistical parameters are R^2, *RMSE,* and *chi-squared* χ^2 [19]. The input data, together with the estimated effective diffusivities and the statistical analysis for every continuous drying case are shown in tab. 2.

Table 2. Calculation data, results and statistics data

Exp. no.	r [mm]	v [ms^{-1}]/ T [°C]	t [minute] to achieve 8%$_{d.b.}$	k [min^{-1}]	D_{eff} [m^{2}min^{-1}]	R^2	RMSE	χ^2
1	13.9	1 / 30	2010	0.00143	$2.80\cdot10^{-8}$	0.9920	0.0246	0.0006
2	14.0	3 / 30	1460	0.00190	$3.77\cdot10^{-8}$	0.9929	0.0371	0.0014
3	14.5	1 / 40	1120	0.00203	$4.33\cdot10^{-8}$	0.9947	0.0394	0.0016
4	13.9	3 / 40	790	0.00325	$6.36\cdot10^{-8}$	0.9903	0.0423	0.0024

During the referent continuous regime of 40 °C / 3 m/s, the M_e value was achieved in approximately 800 minute, and that is the reason for using the 800 minute basis for the analysis of intermittent regimes. Using the procedure of non-linear regression, the next equation of the Arrhenius-type is obtained, where D_{eff} is expressed in [m^{2}min^{-1}]:

$$D_{\text{eff}} = \left[9.65310^{-4} v^{0.327} \exp\left(-\frac{4413.67}{T}\right)\right]60 \tag{15}$$

Figure 4 shows the diagrams for the experimental data and model curves for continuous drying with different air velocities. The statistical analysis from tab. 2 showed that Newton's thin layer drying (TLD) equation gave the satisfactory results for the relevant experimental data. Since the Newton's model fits well, there is no need to approximate the experimental data with some more complex TLD equation.

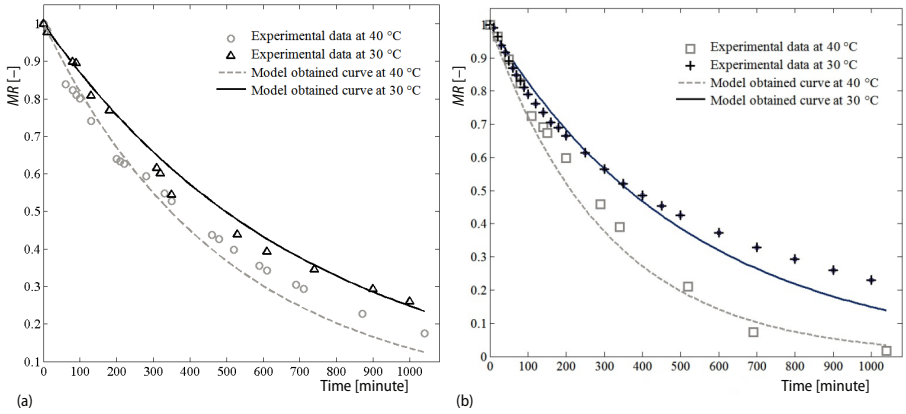

Figure 4. Results for continuous drying; (a) 1 m/s, (b) 3 m/s

After the expression (15) is obtained, the intermittent regime can be modeled by implementing the temperature variation function. Assumed variation of air temperature, together with the measured temperatures and the results for non-stationary heating and cooling of walnuts from eq. (12), are shown in fig. 5. It can be seen that walnut center cools down by almost 80% of the total temperature difference between walnut and hot air in approximately 15 minutes, according to the simulation. On the other side, at [23] it is concluded that for materials in which moisture removal process appears to be faster, material center remains cooler during the process.

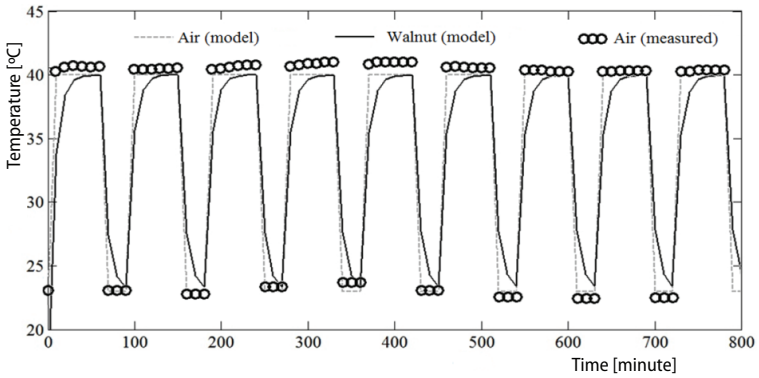

Figure 5. Temperature variation during intermittent drying

Table 3 shows the input data and the statistical analysis for the modeling of intermittent process.

Table 3. Intermittent regimes and statistical data

Exp. no.	r [mm]	v [ms^{-1}]/T [°C]	t [minute]	(t_{on}/t_{off}) [minute]	M_f[%$_{d.b.}$]	R^2	RMSE	χ^2
1	15.3	3 / variable	800	60/30	12.5	0.9955	0.0368	0.0013
2	13.9	3 / variable	800	30/15	7.18	0.9898	0.0350	0.0014
3	14.3	3 / variable	800	variable*	8.00	0.9978	0.0257	0.0006

* The next on/off ratios were used (200 min each): 45/15, 45/30, 45/45, 45/60.

Figure 6(a) shows the diagrams for the experimental data and model curves for intermittent drying with the air velocity at 3 m/s, and variable air temperature, obtained by implementing the regime 60/30, while fig. 6(b) shows the same for the regime 30/15. Figure 6(c) shows the diagrams for variable regime and on fig. 6(d) the drying rates for these three regimes are shown.

It can be noticed that drying curves which are obtained by eq. (15) show the satisfactory results for all three cases. The largest errors appear at the beginning, which could be explained by the fact that drying rates at the beginning of the process are very unpredictable even for the continuous regimes. Further on, for the 60/30 regime drying rate line appears below the continuous drying line most of the time. On the other side 30/15 regime drying rate line lays around the continuous regime line.

Deep bed results

Figure 7 shows the results of deep bed drying simulation. Five different heights are chosen for the illustration. Line waviness caused by intermittency vanishes after 15 cm height.

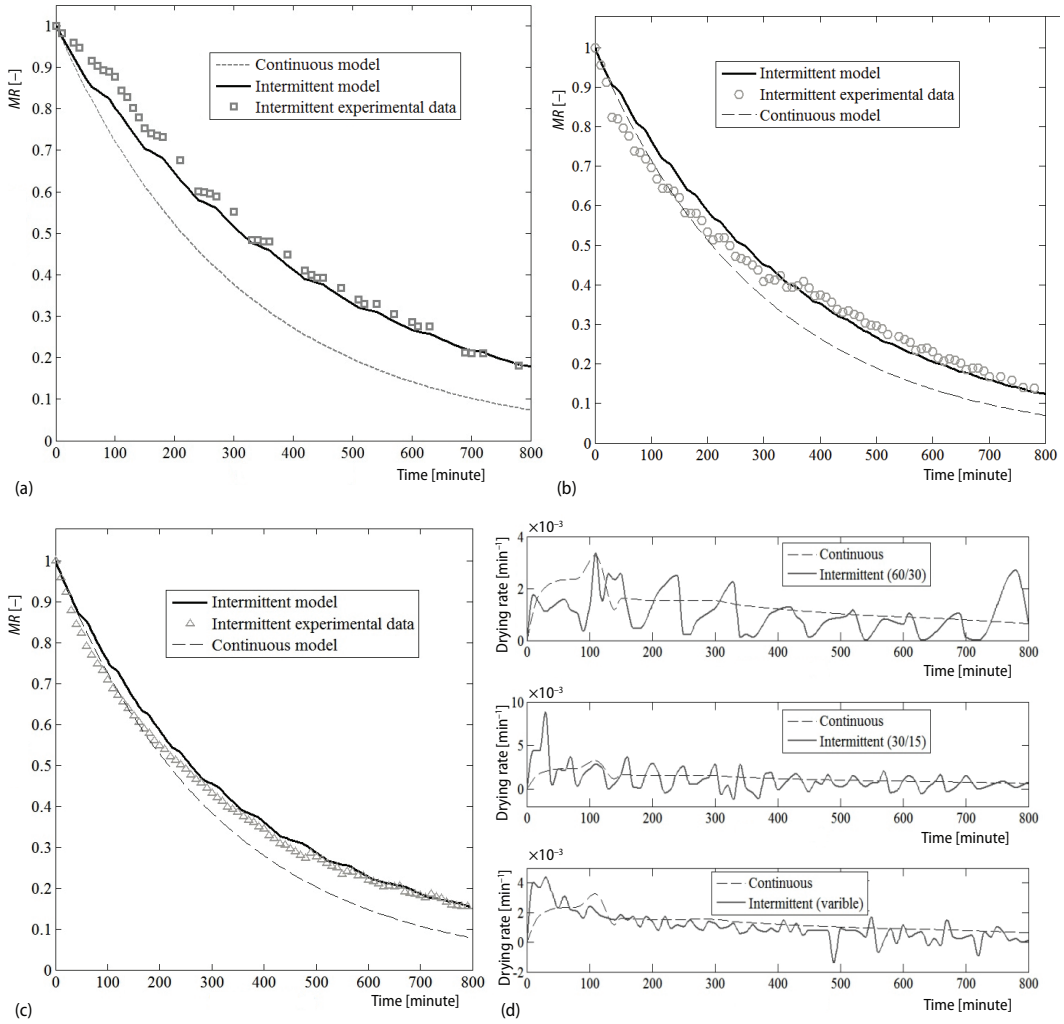

Figure 6. Intermittent drying; (a) 60/30 minute regime, (b) 30/15 minute regime, (c) variable regime, and (d) drying rates

It implies that intermittency does not affect the higher layers. Also, at higher layers, M_e value was not achieved for 1800 minute. Figures 8(a) and 8(b) show the air temperatures and drying rates for each mentioned height, respectively. There can also be seen that for the higher layers temperature variance is practically negligible, hence the drying rate increment after a tempering period is very small.

Conclusions

This investigation deals with the modeling of intermittent drying, so the same time basis was chosen for all experimental cases, in order to prove the model reliability, rather than to achieve the equilibrium moisture content necessarily.

Equation (14) showed good agreement with the experimental data of intermittent regimes, thus it could be used for modeling of intermittent walnuts drying using temperatures and

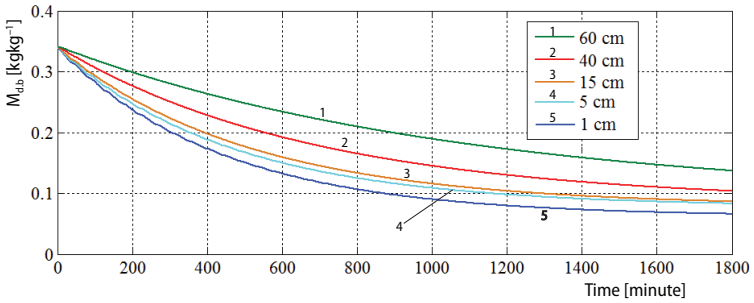

Figure 7. Deep bed intermittent drying curves

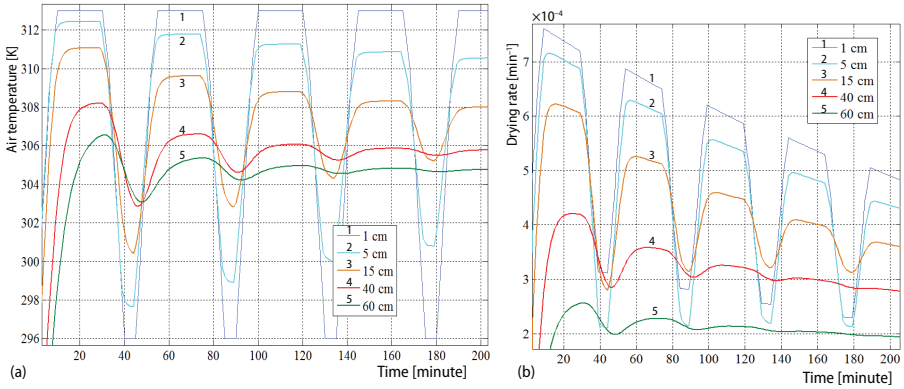

Figure 8. Deep bed intermittent drying; (a) air temperature, (b) drying rates

air velocities equal or lower than 40 °C and 3 m/s. This TLD model could serve as a basis for different deep bed simulations as well.

Besides the obtained energy saving (as a result of the shorter heater work), total drying time extension appears, which is the main problem regarding the intermittent drying application. This makes it more desirable when heater consumes more energy than fan. In other words, it is more suitable for the drying facilities with lower drying capacity (*i. e.* where the smaller amounts of walnuts are dried).

The 30/15 regime achieved the satisfactory final moisture content in 800 minute, unlike the 60/30 regime, so the shorter tempering periods should be preferred. More frequent tempering holds the drying rate value closer to the continuous regime values.

Deep bed drying simulation showed that for the layers higher than approximately 15-20 cm it is more likely that application of intermittent modes will only cause the slower drying process, without any energy savings, since the drying time would be the same as for a process that simply has lower air temperature, thus consumes less energy.

Nomenclature

a,b,c,n – constants, [–]
Bi – Biot number (= $\alpha r/\lambda$), [–]
C_p – specific heat capacity, [kJkg^{-1}K^{-1}]
D – diffusivity, [m^{2}min^{-1}]
d – diameter, [m]
Fo – Fourier number, (= $\lambda t/\rho C_p r^2$), [–]
G – mass flux, [kgm^{-2}s^{-1}]
h_{cv} – volumetric convection coefficient [Wm^{-3}K^{-1}]
k – drying constant, [min^{-1}]
L_g – latent heat of grain moisture
M – moisture content, [%$_{d.b.}$]

MR – dimensionless moisture content (dry basis), [–]
Nu – Nusselt number, [–]
Pr – Prandtl number, [–]
r – effective radius, [mm]
R^2 – coefficient of determination (statistical parameter), [–]
Re – Reynolds number, (= $v^2 r\rho/\mu$), [–]
T – temperature, [°C]
t – time, [min]
v – velocity [ms^{-1}]
X – humidity, [$kgkg^{-1}$]
z – bed height, [mm]

Greek symbols

α – convection coefficient, (= $Nu\lambda/2r$), [$Wm^{-2}K^{-1}$]
Δ – increment, [–]
λ – thermal conductivity, [$Wm^{-1}K^{-1}$]
μ – dynamic viscosity, [Pas]
ρ – density, [kgm^{-3}]
φ – volume fraction, [%]
χ^2 – *chi-squared* (statistical parameter)
ω – mass fraction, [%]

Subscripts

a – air
d.b. – dry basis
e – equilibrium
eff – effective
f – final
g – grain
i – initial
w – water vapor

Acronyms

RMSE – root mean square error (statistical parameter)
TLD – thin layer drying

References

[1] ***, Food and Agricultural Commodities Production, http://www.fao.org/faostat/en/#data/QC
[2] Hassan-Beygi, S.R., *et al*., Drying Characteristics of Walnut (Juglans Regia l.) During Convection Ddrying, *International Agrophysics, 23* (2009), 2, pp. 129-135
[3] Rumsey, T., Thompson, J., Ambient Air Drying of English Walnuts, *Transactions of ASAE, 27* (1984), 3, pp. 942-945
[4] Mamani, I., Modeling of Thermal Properties of Persian Walnut Kernel as a Function of Moisture Content and Temperature Using Response Surface Methodology, *Journal of Food Processing and Preservation, 39* (2015), 6, pp. 2762-2772
[5] Altuntas, E., Erkol, M., Physical Properties of Shelled and Kernel Walnuts as Affected by the Moisture Content, *Czech Journal of Food Science*, *28* (2010), 6, pp. 547-556
[6] Khir, R.,*et al*., Size and Moisture Distribution Characteristics of Walnuts and Their Components, *Food and Bioprocess Technology*, *6* (2013), 3, pp. 771-782
[7] Barbosa de Lima, A. G., *et al*., Drying of Bioproducts: Quality and Energy Aspects, in: *Drying and Energy Technologies* (Eds. Barbosa de Lima AG, Delegado JMPQ), Springer International Publishing, Cham, Switzerland, 2016, pp. 19-42
[8] Motevali, A., *et al*., Comparison of Energy Parameters in Various Dryers, *Energy Conversion and Management*, *87* (2014), Nov., pp. 711-725
[9] Pan, Z., *et al*., Improving Processing and Energy Efficiencies of Walnut Drying, A: Walnut Research Reports, California Walnut Board, Sacramento, Cal., USA, 2009
[10] Hacihafizoglu, O., *etal*., Numerical Investigation of Intermittent Drying of a Corn for Different Drying Conditions,*Thermal Science*, *23* (2019), 2A, pp. 801-812
[11] Kumar, C., *et al*., Intermittent Drying of Food Products: A Critical Review, *Journal of Food Engineering, 121,* (2014), Jan., pp. 48-57
[12] Qu, Q., *et al*., Effects of Three Conventional Drying Methods on the Lipid Oxidation, Fatty Acids Composition, and Antioxidant Activities of Walnut (Juglans Regia L.), *Drying Technology, 34* (2016), 7, pp. 822-829
[13] Baini, R., Langrish, T. A. G., Choosing an Appropriate Drying Model for Intermittent and Continuous Drying of Bananas, *Journal of Food Engineering, 79* (2007), 7, pp. 330-343
[14] Shei, H. J., Chen, Y. L., Computer Simulation on Intermittent Drying of Rough Rice, *Drying Technology, 20* (2002), 3, pp. 615-636
[15] Srivastava, V. K., John, J., Deep Bed Grain Drying Modeling, *Energy Conversion and Management, 43* (2002), 13, pp. 1689-1708
[16] Kowalski, S. J., Pawłowski, A., Energy Consumption and Quality Aspect by Intermittent Drying, *Chemical Engineering and Processing, 50* (2011), 4, pp. 384-390

[17] ***, ASHRAE Handbook (2006): Refrigeration: SI edition, American Society of Heating, Refrigeration and Air-Conditioning Engineers, Atlanta, 2006
[18] ***, AOAC International (2000) Official Methods of Analysis of AOAC International, 17th ed., AOAC International, Gaithersburg, 2000
[19] Balbay, A., *et al*., Modeling of Convective Drying Kinetics of Pistachio Kernels in a Fixed Bed Drying System, *Thermal Science, 17* (2013), 3, pp. 839-846
[20] Akpinar, E., *et al*., Single Layer Drying Behavior of Potato Slices in a Convective Cyclone Dryer and Mathematical Modeling, *Energy Conversion and Management, 44* (2003), 10, pp. 1689-1705
[21] Incropera, F. P., DeWitt, D. P. *Fundamentals of Heat and Mass Transfer,* 4th ed., John Wiley and Sons, New Jersey, USA, 1996
[22] Seshadri, V., Silva Pereira, R. O., Comparison of Formulae for Determining Heat Transfer Coefficient of Packed Beds, *Transactions ISIJ, 26* (1986), Feb., pp. 604-610
[23] Alnak, D. E., Karabulut, K., Computational Analysis of Heat and Mass Transfer of Impinging Jet onto Different Foods during the Drying Process at Low Reynolds Numbers, *Journal of Engineering Thermophysics, 28* (2019), 2, pp. 255-268

Paper submitted: January 20, 2019
Paper revised: May 15, 2019
Paper accepted: May 20, 2019